Progress In Electromagnetics Research C, Vol. 53, 75–87, 2014

A Design of Vehicular GPS and LTE Antenna Considering the Vehicular Body Effects

Patchaikani Sindhuja[1], Yoshihiko Kuwahara[1], Kiyotaka Kumaki[2], and Yoshiyuki Hiramatsu[2, *]

Abstract—In this paper, a vehicular antenna design scheme considering the vehicular body effects is proposed. A wire antenna for GPS and LTE is implemented on the plastic plate, then it is mounted on the front glass. The outputs are commonly used to share the feed. It is necessary for GPS to increase the right hand circularly polarization (RHCP) gain near the zenith and to reduce the axis ratio while for LTE to increase the horizontal and vertical polarization (HP and VP) gain in the horizontal plane. Also for LTE, multiband characteristics are required. In order to achieve the specified performance, the antenna shape is optimized by Parato genetic algorithm (PGA). When the antenna is mounted on the body, the performance is seriously changed. To evaluate performance of the antenna mounted on the body with a complex shape, a commercial electromagnetic simulator (Ansoft HFSS) is used. To apply electromagnetic results output by HFSS to PGA algorithm operating on the MATLAB, MATLAB to HFSS linking program via Visual BASIC (VB) script was used. It is difficult to carry out the electromagnetic analysis with the whole body because of limitations of the calculating load and memory size. To overcome the limitation, we consider only a predominant part where it has an influence on the performance. It is presented that degradations caused by the body are improved through a series of optimization stages. The simulation results obtained clearly show that it is well optimized at 1.575 for GPS and 766.5 MHz and 2.135 GHz for LTE, respectively.

1. INTRODUCTION

Modern vehicles are equipped with a lot of antennas to facilitate a reliable wireless communication that enables a running vehicle to connect with the outside world and tracking geological position system for various applications in addition to basic AM/FM and TV antenna [1]. Existing roof-mounted mast antenna as whip antenna, which has been used for decades to receive radio signals, causes many disadvantages such as easy breakable, wind noise, and limitation of industrial design. Increase in modern automotive radio applications leads to increase in the antenna count installed on the vehicle. In recent years, antenna engineers and researchers have been studying to replace the massive antenna by hidden antennas whose profile does not affect the aesthetic design of the vehicle and does not occupy much space of the vehicle. Also, they have a strong interest in multiband antenna and aperture sharing technology which decreases the number of the antennas and harness.

Glass mounted antennas based on wire geometry formed by using conducting material of a thin thickness, which is laminated between layers of glass in the vehicle windows [2], are suggested to be the best alternative [2]. Recently, a method using the rear glass screen heater as the antenna for reception has been proposed [3]. Glass mounted antennas provide no additional aerodynamic drag and create no wind noise, which is a significant advantage over mast type designs. They also require no holes on

Received 13 June 2014, Accepted 14 August 2014, Scheduled 26 August 2014

* Corresponding author: Yoshihiko Kuwahara (tykuwab@ipc.shizuoka.ac.jp).

[1] Graduate School of Science and Engineering, Shizuoka University, 3-5-1 Johoku, Naka-ku, Hamamatsu 432-8561, Japan. [2] Kojima Industry Co., Ltd., 15 Hirokuden, Ukigai-cho, Miyooshi, Aichi 470-0207, Japan.

the vehicle body, which may lead to cheaper tooling for the metal work. Shared aperture multiband antenna technology is the most promising technology to reduce the antenna count in the vehicular body by combining the functionality of several antenna systems into one single antenna aperture with multiband and multi-polarization performances [4, 5].

Performance of the vehicular antenna is seriously degraded by reflecting and scattering from the body. Since the situation of reflecting and scattering varies according to a car model, many antenna engineers are forced to make great efforts to modify the antenna configuration by experiments. Though the genetic algorithm is widely used to optimize the antenna configuration, we cannot find articles on optimization of the shape considering the platform effects. There is only an article on optimization of the installing position [6].

In the paper, we propose a design scheme of wire antenna design for GPS and LTE installing behind the front glass window. It is known for the RHCP antenna design to mount capacitances on a square loop [7]. In our GPS antenna, stubs are used for capacitance. The position and length of the stubs are optimized by PGA [8–10]. Also LTE antenna of crooked wire [11] that generates HP and VP wave in 700 MHz and 2.1 GHz band is integrated along with the GPS antenna. These feeds are common. Crooked wire shape is also designed by PGA at the same time. On the other hand, it is necessary to consider the performance degradations due to reflecting and scattering caused by the vehicular body. We tried to optimize the antenna shape considering the body effects. Probably, this is the first trial in numerical electromagnetics. In order to model a complicated vehicular body, we used a commercial electromagnetic simulator (HFSS). It is not realistic for an iterative optimization scheme as PGA to analyze the electromagnetic field at the high frequency about the whole vehicular model because of limitations of computing time and memory requirement. Therefore, we consider only a predominant part where it has influence on the performance. PGA algorithm is operating on MATLAB while electromagnetic analysis is carried out on HFSS. Therefore, we have developed an interface which links MATLAB with HFSS [12].

The paper is organized as follows. Section 2 presents our proposed antenna design and its configuration. Section 3 describes the implementation of PGA in antenna optimization combined with HFSS. Section 4 will discuss about the different cases of numerical analysis and numerical results obtained in successive optimizing stages. Finally, Section 5 gives the conclusions of our study.

2. PROPOSED ANTENNA DESIGN

We have a plan to develop the GPS and LTE wire antenna mounted on front glass. From our customers' requirements on LTE, 2 bands of 700 MHz (up-link of 777–787 MHz, down-link of 746–756 MHz) and 2100 MHz (down-link of 2110–2170 MHz) are considered. In 2100 MHz band, only the receiving capability is required. The feeding points are shared in order to use a fed cable in common. Thin metal wire elements for the antenna are printed on a plastic plate. It is necessary for the GPS to receive a circular polarized wave. Loop antenna with a loading reactance whose position and value are properly determined can generate the circular polarized wave. Also, it is necessary for the LTE to transmit and receive both of horizontal and vertical polarized waves in the dual bands. Crooked wire antenna can generate a variety of polarized waves and has broad band capabilities. Configuration of Figure 1 is provided [13] when 2 antennas are mounted on a plastic plate so as to coincide the fed points.

The RHCP wave for GPS band is achieved by varying the side length (A), stub length ($S3, S4$), and stub position ($S1, S2$). The LTE performance is achieved by adding crooked wire made up of straight line segments (Position of the vertex; $L1(x, y)$, $L2(x, y)$, $L3(x, y)$, $L4(x, y)$) on either side of the square loop pattern. Both the loop and wire segments are fed by a common feed point, whose impedance is set to 150 Ω. This value is a requirement of the manufacturer. The antenna pattern is printed on the plastic plate whose size and thickness are 200 mm by 80 mm and 2 mm, respectively. The dielectric constant is 2.5. The perfect conductor of 1 mm width and 0.1 mm thickness is assumed for an antenna element, and it is maintained uniform throughout the design. This compact plastic structure is installed behind the front glass near the rearview mirror.

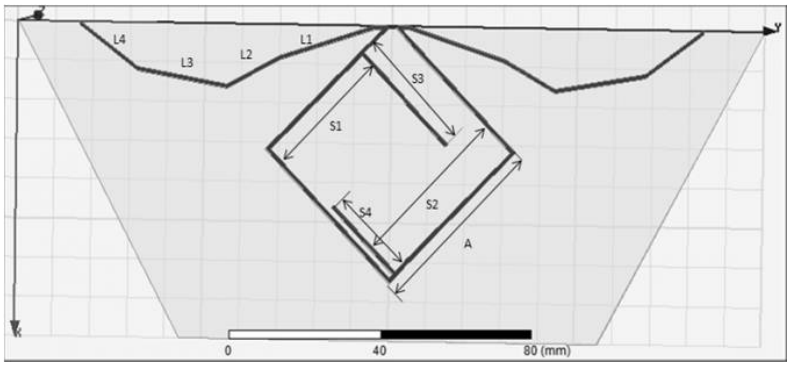

Figure 1. Proposed front glass vehicular antenna design for GPS and LTE band.

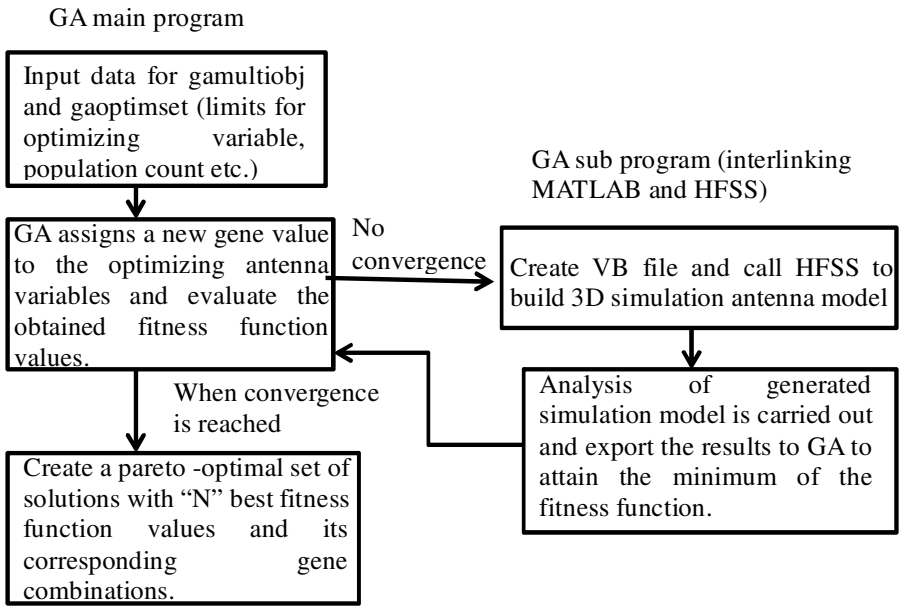

Figure 2. Flowchart for PGA optimization process in our proposed antenna design.

3. GENETIC ALGORITHM (GA) ANTENNA OPTIMIZATION COMBINED WITH HFSS

3.1. Program Flow

Obtaining an optimal antenna design for any particular application is really a challenging task because even a small change in the proposed antenna pattern will affect the antenna performances seriously and it is also not possible to do manual optimization which takes many complex procedures. Hence in our study, PGA in conjunction with a full wave electromagnetic simulator is used to design an optimal gain, impedance, and AR with specified constraints. In our analysis, we used GA multi-objective solver (gamultiobj) provided by MATLAB. The GA main program which includes the input data set for GA optimizer is created. Then, a subprogram is called by passing the values for optimizing antenna variable to create VB file using in built-in MATLAB library functions. Generated VB file then calls HFSS automatically to build the 3D simulation antenna model and perform analysis and then export the simulation results to get the fitness value for GA. GA then assigns a new set of values to the antenna parameters based on the evaluation done on the fitness function values obtained. Hence, the optimized antenna parameters are varied in each step by GA in a manner that the numerical value of targeted fitness function reaches its optimal minimal one.

3.2. Pareto Ranking

This algorithm outputs "N" sets of Pareto-optimal solutions along with their gene combinations. Each optimal solution is a set of values of defined fitness functions, and each gene is a set of optimizing antenna dimensions. An example for Pareto plotting of multi-objective optimization in our numerical analysis is shown in Figure 3 for the generated "6" GA outputs for stage 3 optimization and is also shown in Table 1. Then the gene set corresponding to the optimal solution (6th) is taken as optimized antenna parameters whose dimensions are summarized in Table 6.

Table 1. Generated GA outputs in stage 3 optimization.

FVAL	Obj1 Gain (dB)	Obj2 $r(Z)$	Obj3 AR(dB)
1	−3.02	160	4.28
2	−0.33	192	5
3	−1.01	131	3.9
4	−3.42	118	3.7
5	−0.15	101	4.7
6	0.056	103	3.6

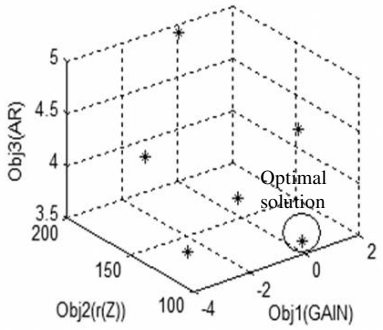

Figure 3. An example of Pareto plot for generated "6" GA outputs in stage 3.

3.3. Fitness Functions Defined in Our GA Optimization and Its Required Specifications

At each iteration, the value of each function defined by Table 2 is evaluated and then processed by GA to achieve the optimal solution for each fitness function. In general, GA works to attain the minimum

Table 2. Fitness function defined for GA optimizer.

SL.NO.	GPS BAND (1.575 GHz)	LTE LOWER BAND (0.7665 GHz)	LTE HIGHER BAND (2.135 GHZ)
Fitness Function 1	RHCP gain > -3 dB ($\Theta = 0°$, Z-axis)	VP gain1 > -3 dB, $\Phi = 90°$ HP gain1 > -3 dB, $\Theta = 90°$	VP gain2 > -3 dB, $\Phi = 90°$ HP gain2 > -3 dB, $\Theta = 90°$
Fitness Function 2	AR< 3 dB at Z-axis		
Fitness Function 3	$r(z1) > 50$ ohm	$r(z2) > 50$ ohm	$r(z3) > 50$ ohm

of the function defined. But in our problem, our aim is to increase the value of fitness functions 1 and 3, and lower the value of fitness function 2. Hence the input to GA solver is,

$$\text{Fval}=[1/\min(\text{RHCP gain, VP gain1, HP gain1, VP gain2, HP gain2}),\ \text{AR},\ 1/\min(r(z1),\ r(z2),\ r(3))] \tag{1}$$

Minimums of the gain of fitness function 1 and impedance of fitness function 3 are found, and their reciprocated values are sent to the GA solver in order to maximize them, and AR is also sent. The important characteristics of antenna are set as fitness functions, and its effectiveness in the antenna design optimization is well shown through the numerical results by next section.

4. NUMERICAL ANALYSIS

We carried out our proposed antenna design in three step by step stages of optimization. The purpose is to observe the influence of vehicular parts, which has major impact on antenna design and to mitigate its effects. Table 3, shown below, will give the outline of antenna optimizing parameters involved and description of simulation model used in each stage of GA optimization. Figure 4 explains the antenna's location on xyz coordinates and definition of the sweep angle. To make GA optimization efficient, it is necessary to set the input parameters values carefully so that the GA does not attain premature convergence. Table 4, shown below, gives the input values used in our optimization program. Elite count specifies the number of individuals that are guaranteed to survive to the next generation. It should be a positive integer, and we set the default value of 2 in our program.

Table 3. Outline of simulation stages in our numerical analysis.

SL.No.	Optimizing antenna parameters and its notation	Case No.	Parts included in the simulation model
STAGE 1	side of square loop, stub length and position, vertex of crookedwire X[13]=[A,S1,S2,S3,S4,L1(x),L2(x),L3(x), L4(x), L1(y),L2(y),L3(y),L4(y)]	1	antenna, plastic plate (Figure 5)
		2	antenna, plastic plate, front glass, front pillar, roof (Figure 6)
STAGE 2	stub length and position, vertex of crooked wire X[12]=[S1,S2,S3,S4,L1(x),L2(x),L3(x),L4 (x), L1(y),L2(y),L3(y),L4(y)]	3	antenna, plastic plate, front pillar (Figure 10)
		4	antenna, plastic plate, front glass, front pillar, roof (Figure 6)
STAGE 3	stub length and position, vertex of crooked wire, antenna position X[13]=[S1,S2,S3,S4,L1(x),L2(x),L3(x),L4 (x), L1(y),L2(y),L3(y),L4(y), d]	5	antenna, plastic plate, front pillar (Figure 16)
		6	antenna, plastic plate, front glass, front pillar, roof (Figure 6)

4.1. Stage1: GPS and LTE Antenna Design Attached with Plastic Substrate [12]

In stage 1, a proposed antenna configuration attached on the plastic substrate is optimized based on Figure 1. Three frequency points of 0.7665, 1.575, and 2.135 GHz are set and analyzed. They are middle frequencies of LTE lower frequency band (0.746–0.787 GHz), GPS bandwidth (1.475–1.675 GHz), and LTE higher frequency band (2110–2170 MHz). To achieve GPS performance, the RHCP gain at bore sight is processed to maximize at the frequency while the corresponding AR is processed to minimize

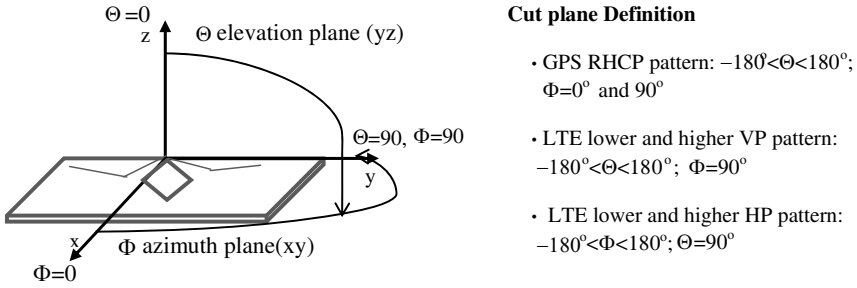

Figure 4. Proposed antenna in xyz co-ordinate and its analyzing cut planes.

Table 4. Input parameter set for GA optimizer.

Population size	30
Number of generation	15
Cross over fraction	0.85
Elite count	2
Number of optimizing variable	13 in case1 and 5, 12 in all other cases
Fitness function	3

(< 3 dB). Of course, the impedance must be matched with 150 Ω. In the case of LTE, the VP and HP gains at the specified angle are processed to maximize at the dual frequency points while the impedance must be matched with 150 Ω.

4.1.1. Simulation Results for CASE1 and CASE2

An optimized antenna configuration is shown in Figure 5. The details of the dimensions are summarize in Table 6. Then, it is mounted on a vehicular body as shown in Figure 6 to study the influences of vehicular body. We call the antenna before mounting the body as "case 1", and that after mounting the body as "case 2".

The 2D RHCP radiation pattern at GPS band (1.575 GHz) for cases 1 and 2, VP and HP 2D radiation patterns at LTE bands(0.7665 and 2.135 GHz) for cases 1 and 2, with respect to Figure 4 are shown in Figures 7 and 8, respectively. Figure 7(a) (case 1) has good GPS 2D characteristics such as high gain, low backlobe and bandwidth. However, when we attach it to the vehicular body, these characteristics degrade seriously as shown in Figure 7(b) (case 2). Backlobe and distortion become larger. It is seen from Figures 8(a) and (c), LTE bands 2D patterns are similar to the dipole patterns. However, when we attach the antenna to the vehicular body, as GPS pattern, LTE patterns also degrade, and the VP peak gain at the lower band decreases drastically.

Inclusion of vehicular body also influences the impedance of antenna, and it is observed by plotting the frequency versus the real part of impedance calculated for cases 1 and 2 as shown in Figure 9.

4.2. Stage 2: Optimization of GPS and LTE Antenna Pattern Attached with Plastic, Front Pillar and Front Glass

In order to control the vehicular body effects on the proposed antenna design, in stage 2 of the antenna design optimization, front glass (thickness 5 mm and its dielectric constant is 8.2) and front pillar (metal of thickness 1 mm) are also considered as shown in Figure 10. Inclusion of roof will enlarge the simulation model, and corresponding absorption boundary and leads to very long simulation time. Therefore, roof part of vehicle is excluded. To confirm the roof effects, it was attached after the optimization.

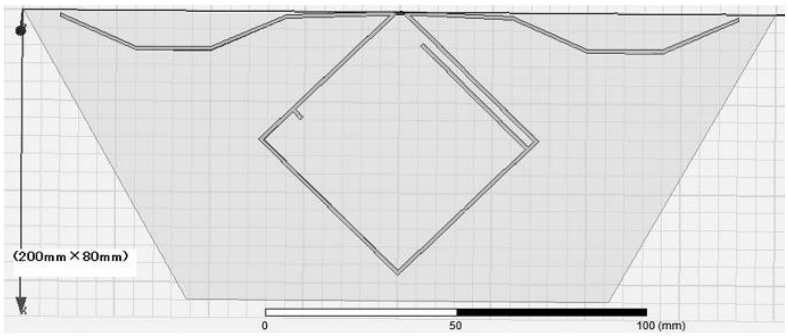

Figure 5. Case 1 simulation model with stage1 optimized antenna pattern.

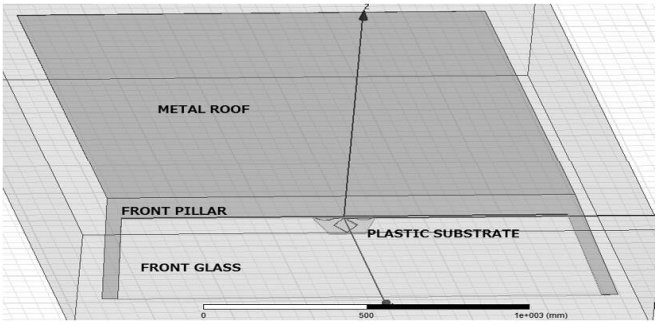

Figure 6. Case 2 simulation model.

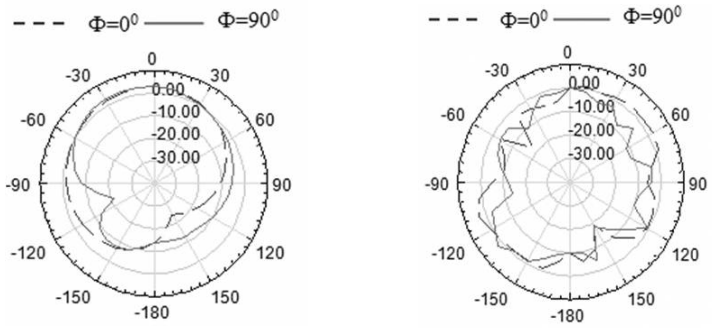

(a) case1 (b) case2

Figure 7. 2D RHCP patterns of the stage 1 optimized vehicular antenna at GPS band.

4.2.1. Simulation Results for Case 3 and Case 4

The detailed configuration of stage 2 optimized antenna pattern is shown in Figure 11. The details of the dimensions are summarized in Table 6. We call the optimized antenna pattern obtained in stage 2 before attaching the roof as "case 3" and that after attaching the roof as "case 4" (See Figure 12).

The 2D RHCP radiation pattern at GPS band (1.575 GHz) and HP and VP 2D radiation patterns at LTE bands (0.7665 GHz and 2.136 GHz) are shown in Figures 13 and 14, respectively.

Case 4 results have close similarities to case 3 (i.e., the performance of case 3 antenna was not degraded even after attaching the roof), whereas case 1 antenna results get degraded badly when roof was attached. Thus the effectiveness of stage 2 optimization over stage 1 optimization is confirmed and is well shown in Figures 13 and 14. The peak gain of RHCP and LTE HP, VP gain get improved. Though stage 2 produces better results than stage 1, distortions still exist in RHCP GPS pattern, and the LTE lower band impedance is too low to execute shown below.

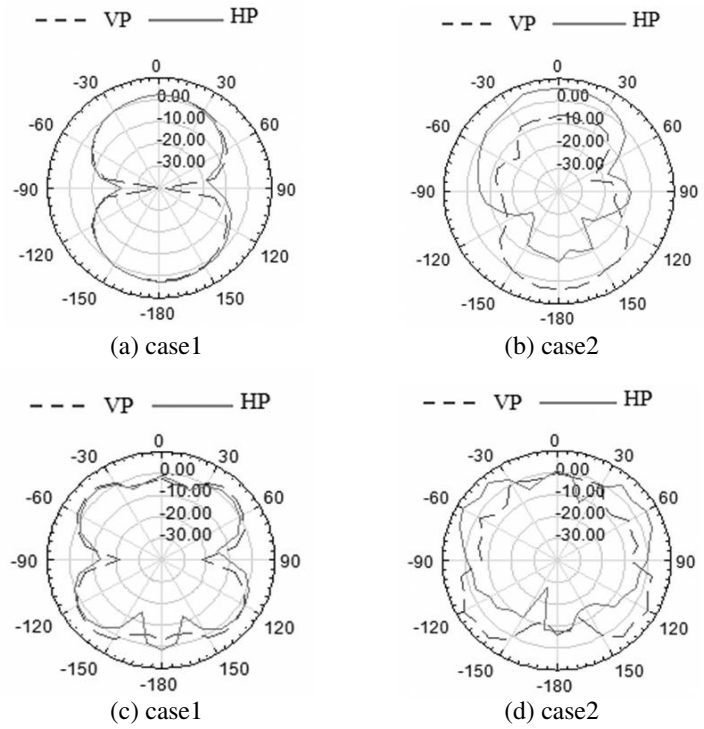

Figure 8. 2D HP and VP patterns of the stage 1 optimized vehicular antenna at LTE (a), (b) lower and (c), (d) higher bands.

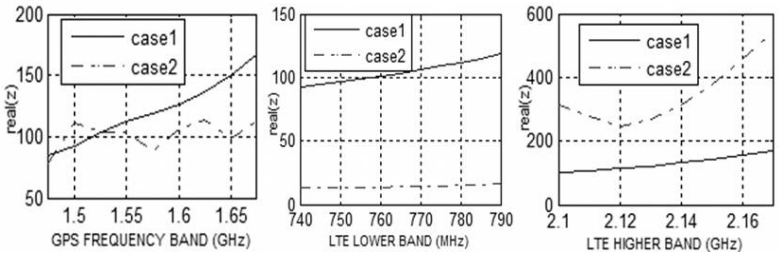

Figure 9. Impedance band characteristics of stage 1 optimized vehicular antenna in all bands.

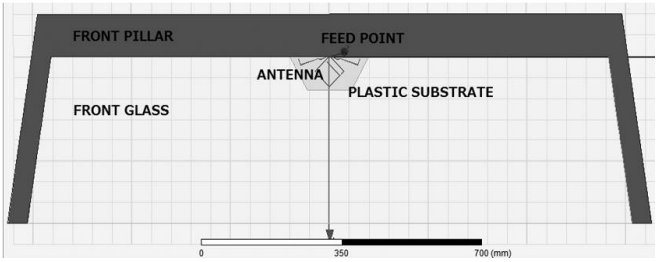

Figure 10. Case 3 simulation model with stage 2 optimized antenna pattern.

4.3. Stage 3: Optimization of GPS and LTE Antenna Pattern Attached with Plastic, Front Pillar and Front Glass by Varying Antenna Position along the Substrate

We observe that the antenna is located very closely to the metal roof and front pillar of the vehicular body which badly influences the current distribution of antenna. So, in this third stage of optimization we are going to optimize the position of entire antenna pattern by varying along the plastic plate's

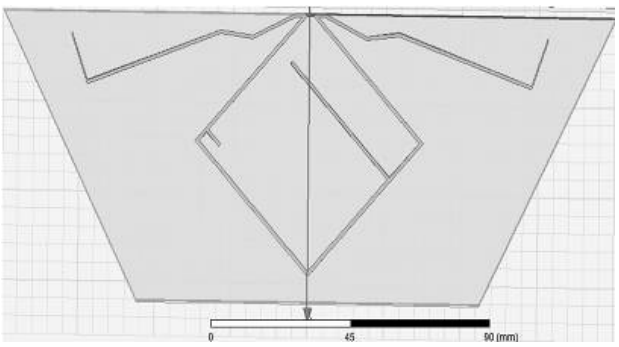

Figure 11. "Stage 2" detail optimized antenna aperture.

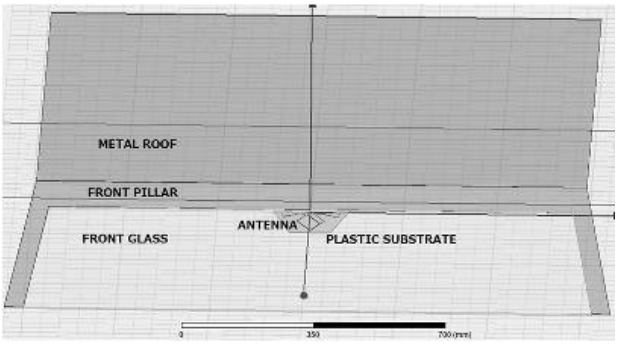

Figure 12. Case 4 simulation model.

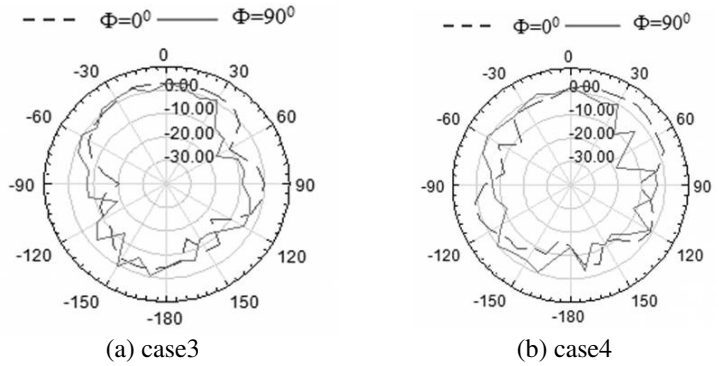

(a) case3 (b) case4

Figure 13. 2D RHCP patterns of the stage 2 optimized vehicular antenna at GPS band.

height in addition to the above mentioned optimizing antenna parameters. To have a free movement of antenna, the plastic plate height is enhanced from 80 mm to 120 mm as shown in Figure 16, and the length remains the same.

4.3.1. Simulation Results for Case 5 and Case 6

We call the optimized antenna pattern obtained in stage 3 before attaching the roof as "case 5" and that after attaching the roof as "case 6". The RHCP 2D radiation patternat GPS band (1.575 GHz) and HP and VP 2D radiation pattern at LTE lower (0.7665 GHz) and higher (2.135 GHz) bands are shown in Figures 17 and 18, respectively.

By comparing Figure 17 and Figure 18 with Figures 13 and 14 and also with Figures 7 and 8 correspondingly, it is clearly shown that stage 3 optimization is very effective, minimizes the distortions and improves the overall antenna performances at both GPS and LTE band. Stage 3 optimized antenna impedance band characteristics is shown in the following Figure 19. The impedance plots of stage 3 optimization clearly show that the antenna has achieved good impedance matching. GA effectiveness in impedance improvement is confirmed by comparing Figure 19 with Figures 15 and 9.

4.3.2. Summarized Data of Proposed Antenna in All Simulation Cases

Table 5, shown below, summarizes the optimal output of GA optimization in each stage.

Comparing case 2 and case 4 data from Table 5, it is clearly shown that the antenna performance under vehicular body part's influence is improved after the second stage of optimization (i.e., magnitude of impedance is improved and gain improved overall in all the bands except the VP gain at LTE higher band). Axis ratio gets drastically reduced from 35 dB to 6.8 dB which is better for GPS antenna.

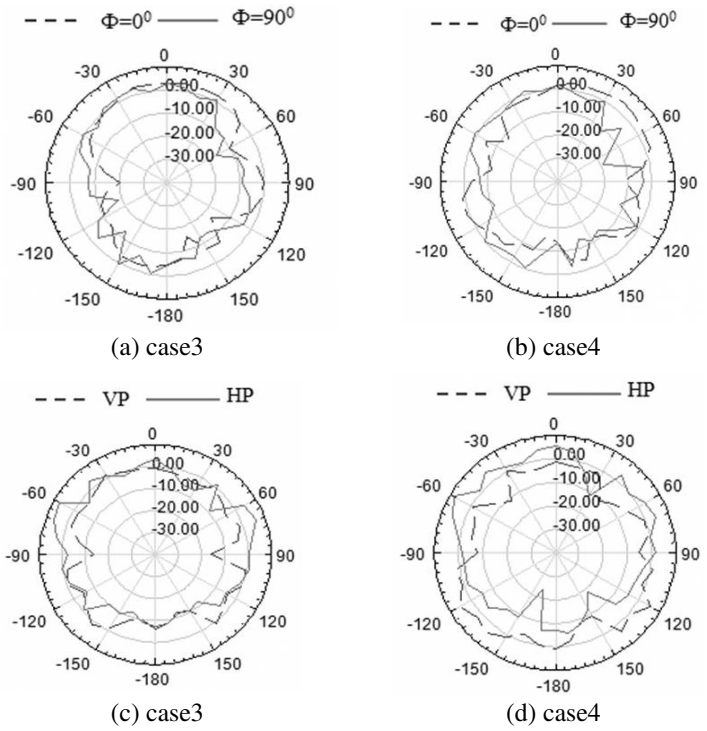

Figure 14. 2D HP and VP patterns of the stage 2 optimized vehicular antenna at LTE (a), (b) lower and (c), (d) higher bands.

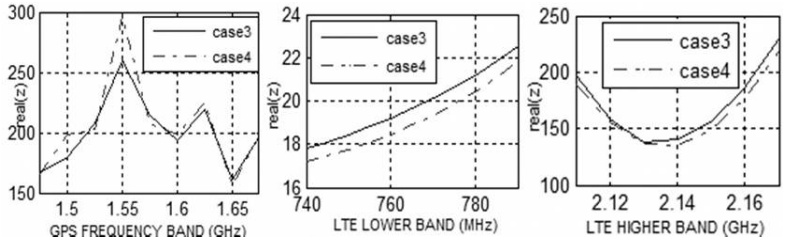

Figure 15. Impedance band characteristics of stage 2 optimized vehicular antenna in all bands.

Figure 16. Case 5 simulation model with stage 3 optimized antenna pattern.

The value shown in Table 5 for case 5 and case 6 antennas clearly shows its improvement of overall performance.

Along with the fitness function values, GA also outputs its corresponding gene combination (i.e., optimized antenna parameters). Table 6 shows the detailed dimensions of each optimized antenna configuration given by each stage of optimization.

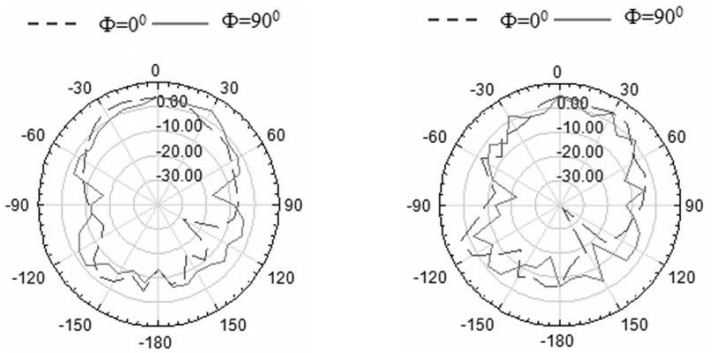

(a) case5 (b) case6

Figure 17. 2D RHCP patterns of the stage 3 optimized vehicular antenna at GPS band.

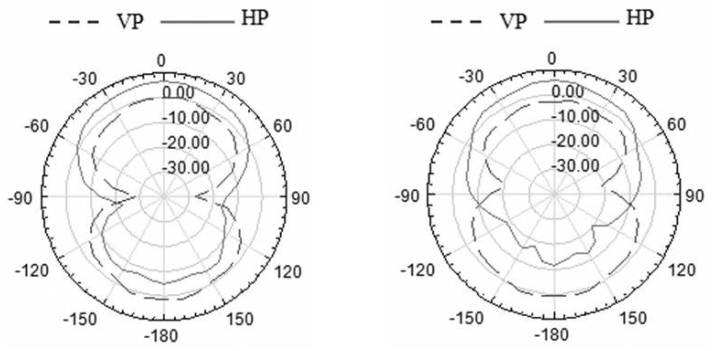

(a) case5 (b) case6

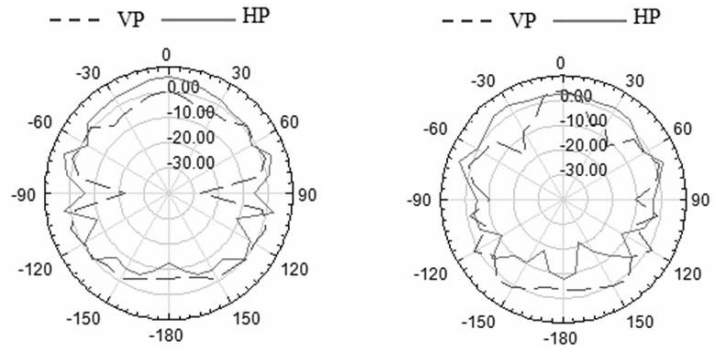

(c) case5 (d) case6

Figure 18. 2D HP and VP patterns of the stage 3 optimized vehicular antenna at LTE lower (a), (b) and higher bands (c), (d).

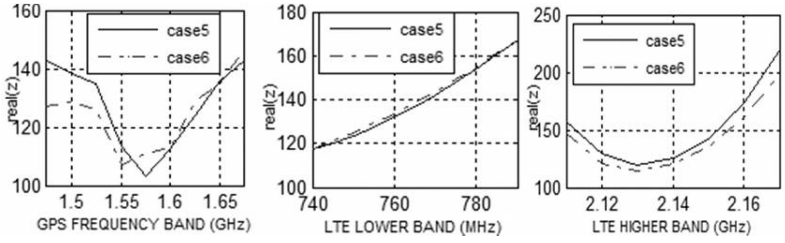

Figure 19. Impedance band characteristics of stage 3 optimized vehicular antenna in all bands.

Table 5. Summarized proposed antenna performances in each case.

Case	Radiation Resistance (ohm)			Gain (dBi)					AR (dB) 1.575 GHz
	766.5 MHz	1.575 GHz	2.135 GHz	766.5 MHz		1.575 GHz	2.135 GHz		
				VP	HP		VP	HP	
1	104.1	119	126	2.3	2.1	2.9	−2.4	−1.4	2.8
2	13.9	87.9	290	−6.1	5.7	−0.1	−0.3	1.3	35
3	19.7	214	138	−1.9	6.8	2.6	−0.1	3.5	3.6
4	19	207	134	−5.3	5.8	1.8	−1.1	5.8	6.8
5	138.2	103	121	0.06	6.5	4.1	0.7	6.4	3.6
6	139.9	111	116	−2.7	5.8	4.7	4.4	2.7	3.1

Table 6. Summarized optimized antenna dimensions in each stage (Unit: mm).

STAGE	A	S1	S2	S3	S4	L1 (x)	L2 (x)	L3 (x)	L4 (x)	L1 (y)	L2 (y)	L3 (y)	L4 (y)	d
1	52.8	12.8	3	3	40	1	10	10	1	70	50	30.1	10	-
2	52.8	5.33	14.51	5.72	45.13	6.28	4.98	19.31	5.95	81.36	70.78	27.43	22.26	-
3	52.8	6.8	3	5.72	38.97	3.32	14.64	12.8	2.66	86.29	60.32	33.25	18.96	43.82

5. CONCLUSION

A vehicular GPS and LTE antenna design considering body effects is proposed in this paper. In the first stage of analysis, GPS performance is achieved by forming square loop pattern with stubs, and LTE performance is achieved by adding crooked wire segments on either side of the loop with common feed point, using the Pareto GA. In the second stage of analysis, influence of front pillar and front glass over the antenna performances is well studied and then further optimization process is carried out by including front pillar and front glass. From the 2D plots in case 4, it is observed that the radiation plots of RHCP pattern for GPS band have been improved by making the main beam lobe wider and suppress the back lobe. However, the LTE bands gain must be improved. So we conduct the third stage of analysis, by optimizing the antenna position from the roof. Case 5 and case 6 data in Table 5 clearly show that the GA obtained its best optimal solution for the proposed design. Since we cannot model and simulate the whole vehicular body in HFSS-EM simulator, due to its large volume, we next plan to implement this GA numerical analysis by interlinking xFDTD and MATLAB to study the antenna performance under the whole vehicular body.

REFERENCES

1. Rabinovich, V., N. Alexandrov, and B. Lkhateeb, *Automotive Antenna Design and Applications*, ISBN978-1-4398-0407, CRC Press, March 18, 2010.
2. Jensen, W. K., "Concealed windshield broadband antenna," U.S. Pat. 3,576,576, 1971.
3. Abdullah, N. and Y. Kuwahara, "VHF adaptive antenna using a rear defogger," *IEEE Trans on Antennas and Propagat.*, Vol. 60, No. 3, 1228–1236, 2012.
4. Wang, J. J. H. and V. K. Tripp, "Conformal multifunction shared-aperture antenna," U.S. Patent No. 5,508,710, 1996.
5. Wang, J. J. H., "Conformal multifunction antenna for automobiles," *2007 International Symposium on Antennas and Propagation*, 234–237, 2007.
6. Infantolino, J. K., M. J. Barney, and R. Haupt, "Optimal position for an antenna using a genetic algorithm," *Proc. of MILCOM 2009 IEEE*, 1–6, 2009.

7. Tokumaru, S. and S. Okubo, "Loaded loop antennas for circular polarization," IEICE Tech. Report, AP81-33, 1981.
8. Rahmat-Samii and E. Michielssen, *Electromagnetic Optimization by Genetic Algorithms*, ISBN 0-471-29545-0, Wiley Interscience, 1999.
9. Kuwahra, Y., "Multiobjective optimization design of Yagi-Uda antenna," *IEEE Trans on Antennas and Propagat.*, Vol. 53, No. 6, 1984–1992, 2005.
10. Maruyama, T., K. Yamamori, and Y. Kuwahara, "Design of multibeam dielectric lens antennas by multi-objective optimization," *IEEE Trans. Antennas and Propagat.*, Vol. 57, No. 1, 57–63, 2009.
11. Altshuler, E. E., "Wire-antenna designs using genetic algorithm," *IEEE Antennas and Propagation Magazine*, Vol. 39, No. 2, April 1997.
12. Patchaikani, S. and Y. Kuwahara, "GA optimization of transparent MIMO antenna for smartphone," *IEICE Electronics Express*, Vol. 10, No. 11, 1–8, 2013.
13. Patchaikani, S. and Y. Kuwahara, "Vehicular loop antenna design for GPS and LTE applications," *General Conference on Electric Society Tokai Branch*, K5-1, 2013.